

# Devices for solar driven water splitting to H<sub>2</sub> fuel and their technical and economic assessments

Richard Foulkes, Chaoran Jiang and Junwang Tang

Department of Chemical Engineering, University College London, Torrington Place, London,

WC1E 7JE (UK)

*Email: Junwang.tang@ucl.ac.uk*

**Table of Contents**

1. <i>Introduction</i> .....	3
2. <i>Fundamental knowledge of water splitting</i> .....	4
2.1 Water Splitting Chemistry .....	4
2.2 PV-electrolysis of Water.....	4
2.3 Photocatalytic and PEC Water Splitting .....	6
3. <i>Technical and Economic Assessments</i> .....	10
3.1 PV-electrolysis of Water.....	10
3.1.1 Technology Drivers .....	10
3.1.2 Plant Operability .....	11
3.1.3 Techno-economic Findings.....	13
3.2 Photocatalytic and PEC Water Splitting.....	16
3.2.1 Technology Drivers .....	16
3.2.2 Plant Operability .....	17
3.2.3 Techno-economic Findings.....	20
4. <i>Material development for PEC water splitting</i> .....	26
4.1 Photoanode materials .....	26
4.2 Photocathode materials .....	28
4.3 Co-catalyst selection .....	30
5. <i>Conclusion</i> .....	32
<i>References</i> .....	33

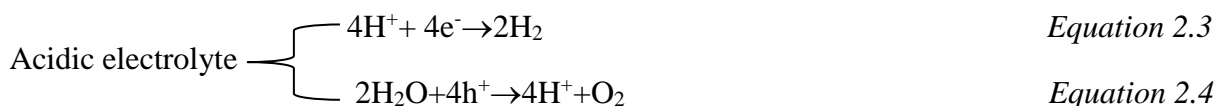
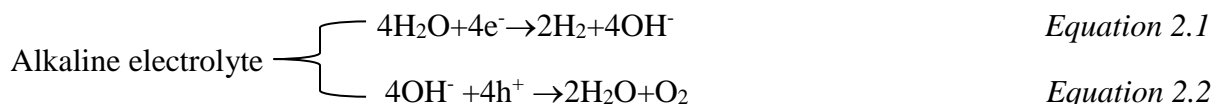
## ***1. Introduction***

With the growing technology advances as well as the ever increasing population in this booming world, the global energy consumption rate is expected raised by a factor of two, from 15 TW/year today to 27 TW per/year by 2050 and according to this trend, it further increase to 43 TW/year by 2100.<sup>1</sup> At present, the main energy supply is obtained from the combustion of fossil fuels, contributing 85% of the total global energy.<sup>2</sup> However, the upcoming depletion of fossil fuels and linked environmental issues such as pollution and greenhouse gases emission while burning them are the biggest technological challenges being encountered by mankind. Therefore, it is imperative to seek an alternative energy supplies to cope with the problem of energy crisis and climate change. Each year, solar energy reaches to the earth surface at the annual rate of 100,000 TW of energy, out of which, 36,000 TW is on land. This means only 1% of the land is needed to be covered with 10% PEC cells to generate the energy of 36 TW/year, which is sufficient for the annual energy consumption in 2050.<sup>2</sup> Hence, the ability of utilizing solar energy is of great importance for humans. Solar energy can be harvested by using PV cells, photocatalysis and photoelectrochemical (PEC) cells to produce hydrogen from water. Hydrogen possesses attractive advantages such as environmental friendly and minimum 3-4 folders higher mass energy density compare to other fossil fuels.<sup>3</sup> Among these three technologies to split water, PV-electrolysis utilizes electricity generated through a coupling with solar photovoltaic (PV) cells to split water in an electrolyser. Photocatalytic and PEC water splitting belongs to the direct solar water splitting branch of hydrogen production technologies. Direct solar technologies use incident sunlight to drive the splitting process and are commonly applied using two different system architectures. One system uses photoactive particles suspension on the surface of which reactions occur. The other uses either photocathode or photoanode to produce H<sub>2</sub> and O<sub>2</sub> separately (PEC cells). This review is going to compare these three technologies in terms of economy and feasibility and then detail the most suitable technology for future hydrogen generation by solar-driven water splitting.

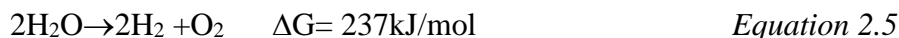
## 2. Fundamental knowledge of water splitting

### 2.1 Water Splitting Chemistry

Water splitting reaction is an uphill reaction, which requires minimum Gibbs free energy of 237 kJ/mol. The reaction half reactions are different depending on whether the electrolyte used is alkaline (Equation 2.1 and 2.2) or acidic (Equation 2.3 and 2.4).



Therefore, the overall water splitting reaction can be expressed as equation 2.5, and the potential difference ( $\Delta V$ ) between water oxidation and reduction reaction is 1.23V, which is also the minimum thermodynamic requirement of solar driven water splitting.



### 2.2 PV-electrolysis of Water

PV-electrolysis combines the electrochemical principals of electrolysis with the photochemical utilisation of incident solar energy. In the electrolysis process a direct current is circulated through water between two electrodes (the anode and the cathode) physically separated by a diaphragm or membrane.<sup>4</sup> The electrodes are submerged in water, often with an electrolyte which increases the ionic conductivity. An oxidation reaction occurs on the anode, generating oxygen and causing electrons to flow on to the external circuit - leaving the anode positively charged. The electrons flow to the cathode negatively polarizing the electrode and producing hydrogen through a reduction reaction. The two half-reactions combine to give the overall water splitting reaction. Separating the electrodes serves to prevent the recombination of hydrogen and oxygen thereby minimising loss of solar energy. A graphical representation of general electrolysis processes is shown in Figure 2.1.

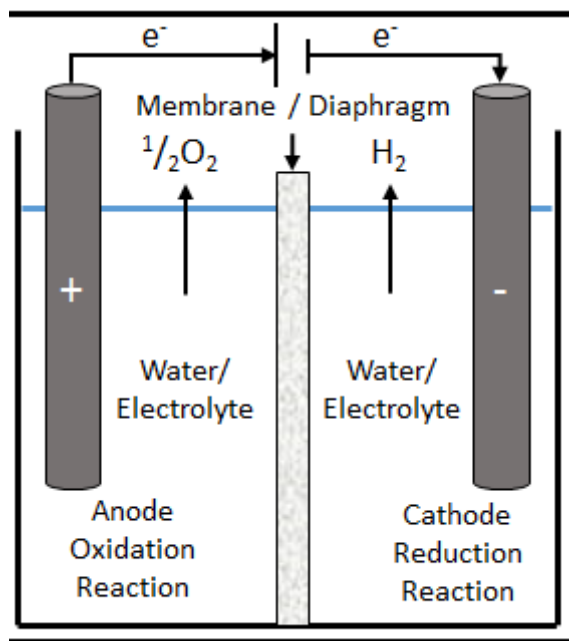


Figure 2.1 : General representation of electrolysis processes

Figure 2.2 (a) shows how the two systems are coupled in an autonomous layout. As the more mature technologies, hybrid systems involving alkaline<sup>5-8</sup> and PEM<sup>9-13</sup> electrolyzers have been the focus of much of the research in this area. However work on solid-oxide electrolyzers has also been carried out providing a proof of concept.<sup>14, 15</sup>

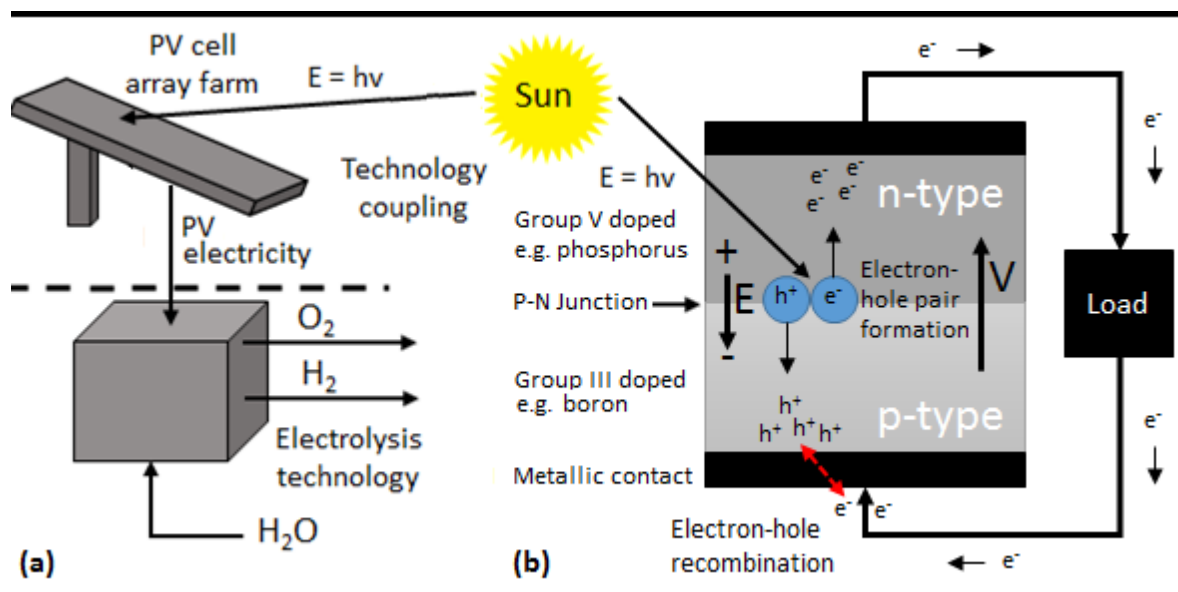


Figure 2.2 : (a) PV electricity and electrolysis technology coupling; (b) Photovoltaic cell operation.

Many textbooks provided a detailed explanation of the principles and mathematics behind photovoltaic cells.<sup>16-19</sup> A general overview of the operation principles will however briefly be covered here (Figure 2.2 b). The most common types of photovoltaic cells are made using semiconductor materials in crystal lattices such as silicon. The lattices are doped with a species that, relative to silicon, are either electron rich or electron deficient - becoming what is known as n-type and p-type materials respectively. When these two materials are brought together they form a P-N junction. The relative difference in electron distribution causes diffusion of electrons from the n-side of the junction across to the p-side. Similarly holes, attracted to the negative charge, move in the opposite direction from the p-side to the n-side. This charge movement establishes an electric field,  $E$ , which builds until it balances the flow. However the flow is balanced by the electric field acting in the opposite direction. To do this the field must attract negatively charged electrons to the n-side and positively charged holes to the p-side. Therefore when incident light rays with sufficient photon energy create electron-pair holes, liberated electrons move to the n-side and holes move to the p-side. The separation of these electrons and holes creates a potential,  $V$ . When the n-type material is connected via an external load to the p-type material, liberated electrons are attracted by the positive charge and are drawn through. An electric current is thus generated. The electrons reaching the p-type material recombine with the migrating holes, hence restoring charge neutrality. If the external load is the water electrolysis system, electricity generated by the solar cell is utilised to drive water splitting, thus storing solar energy into  $H_2$  fuel.

### ***2.3 Photocatalytic and PEC Water Splitting***

Technically, a photocatalytic reaction (suspension system) includes three main processes as shown in Figure 2.3. Firstly, it begins with the absorption of a solar photon in a semiconductor material to form an excited electron-hole pair (Figure 2.4). In order to achieve photocatalytic water splitting using a single semiconductor, the electrons in the conduction band (CB) must have more negative potential than 0 V (vs NHE at pH=0) to conduct the water reduction reaction and the holes in the valence band (VB) must have more positive potential than 1.23V (vs NHE at pH=0) to conduct the water oxidation reaction (Figure 2.4). On this basis minimum band gap energy of 1.23eV is required. In practice, larger band energies are required to drive photocatalytic reactions due to energy losses associated with the over potentials of water

reduction and oxidation reactions.<sup>20</sup> The second process is the charge separation and transportation (Figure 2.3). Since photo-generated electron-hole pairs will easily recombine before migrating to surface, in a photocatalytic reaction, sacrificial reagents are commonly employed. For example, a hole scavenger such as triethanolamine<sup>21</sup> or methanol<sup>22</sup> can be used in the water reduction half reaction to produce hydrogen. Similarly an electron scavenger such as silver nitrate<sup>23</sup> can be used in the water oxidation half reaction to generate oxygen. The third process is the surface chemical reaction. In order to facilitate the charge separation and surface reaction, photocatalysis is often modified with appropriate co-catalyst.

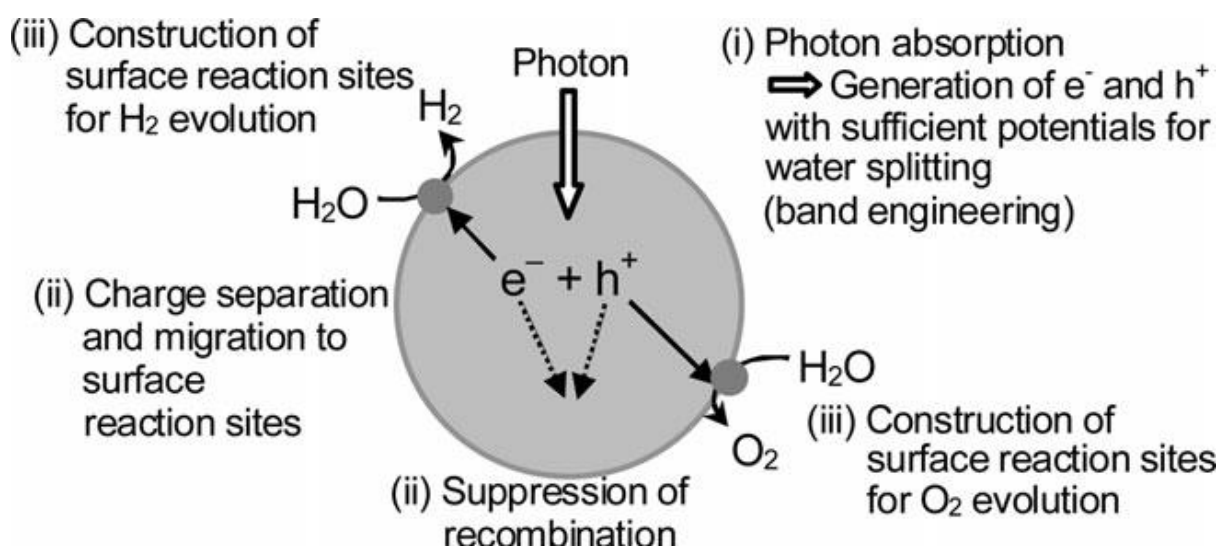
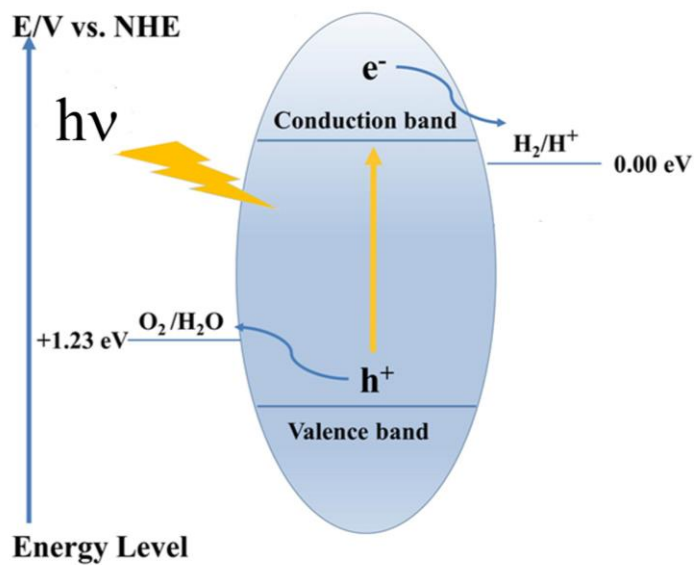


Figure 2.3 : Three processes in photocatalytic water splitting. Reproduced from Ref. 24 with permission from The Royal Society of Chemistry.



*Figure 2.4 : Photocatalytic water splitting through single semiconductor*

The main component of PEC water splitting devices is semiconductor photoelectrodes instead of photocatalyst powder. In addition an electrolyte is necessary. As shown in Figure 2.5, similar to photocatalytic reaction, a complete PEC water splitting reaction contains three processes as well. However, in a PEC configuration, an electrical bias is used to assist electron-hole separation. In addition,  $O_2$  and  $H_2$  can be produced separately on two different electrode surfaces in a PEC water splitting system.



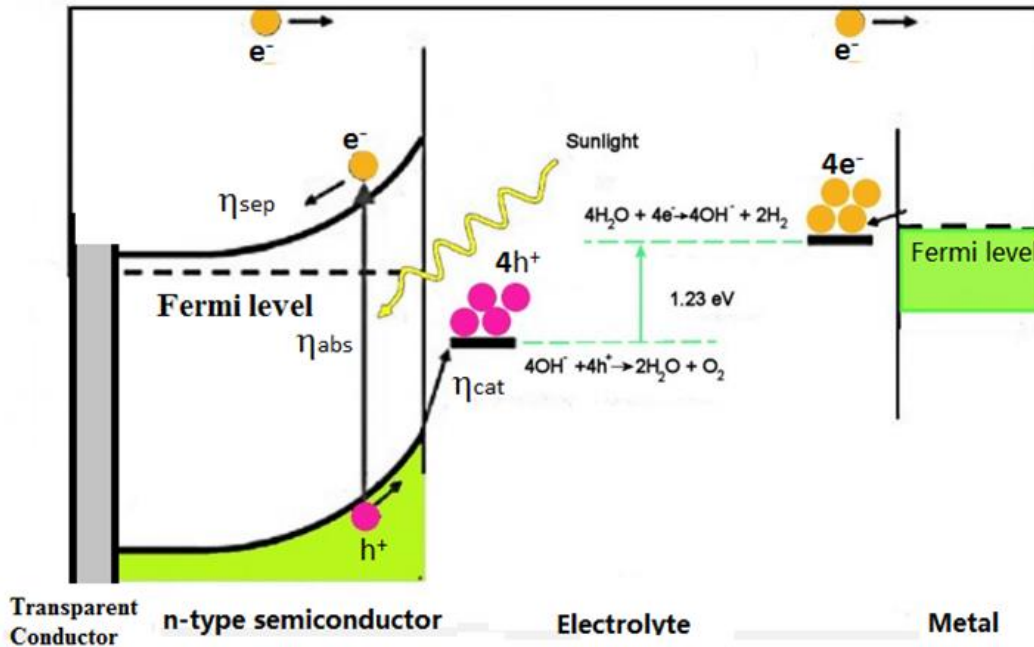


Figure 2.5 : Schematic diagram of a simple PEC cell and three involved processes

The overall efficiency (Solar to Hydrogen Efficiency) of a PEC water splitting cell is limited by the efficiency of each step. Therefore, the solar to hydrogen ( $\eta_{STH}$ ) efficiency can be expressed as the following equation:

$$\eta_{STH} = \eta_{abs} \eta_{sep} \eta_{cat} \quad \text{Equation 2.6}$$

STH efficiency can also be defined as the ratio of total energy generated and total energy input by sunlight illumination:

$$\eta_{STH} = \frac{\text{Total energy generated}}{\text{Total energy input}} = \frac{\Delta G \times R_{H_2}}{P \times A} \quad \text{Equation 2.7}$$

Where  $\Delta G$  is the Gibbs free energy (237KJ/mol);  $R_{H_2}$  is the rate of Hydrogen production in mole/s;  $P$  is the light intensity (100mW/cm<sup>2</sup>) and  $A$  is the illuminated area of the photoelectrode (cm<sup>2</sup>).

However, in most cases, the following equation is used to calculate the STH in a PEC cell <sup>25</sup>:

$$\eta_{STH} = \frac{P_{out} - P_{in}}{P_{light}} = \frac{j_{ph} (V_{redox} - V_{bias})}{P_{light}} \times \eta_{faraday} \quad \text{Equation 2.8}$$

Where  $V_{redox}$  is the redox potential for water splitting (1.23V vs NHE);  $V_{bias}$  is the applied bias added between working electrode and reference electrode;  $P_{light}$  is light intensity

(100mW/cm<sup>2</sup>);  $\eta_{\text{faraday}}$  is the faraday efficiency.  $J_{\text{ph}}$  is the generated photocurrent density.

### ***3. Technical and Economic Assessments***

Although these processes have the common goal of splitting water into hydrogen and oxygen, the economics of each technology is influenced by distinctly different factors. PV-electrolysis depends on developments in photovoltaic cells - both price and efficiency. Photocatalytic and PEC water splitting depend on the reactor design and material development. Although this assessment considers a well-to-gate basis, it is worth pointing out that formidable post-processing challenges still remain for solar generated fuels such as hydrogen. Notable hurdles include the storage and transportation of hydrogen as well as safe and commercially viable utilization in fuel cells. Work in these areas is ongoing with incremental improvements driving progress.

#### ***3.1 PV-electrolysis of Water***

The economics of PV-electrolysis is very similar to that of grid electrolysis. However because the electricity is generated 'in house' with a PV panel, the economics are not as strongly correlated to the grid electricity price. Economic feasibility is a function of the performance of the system (PV cells and electrolysis units together). This means an improvement in the PV technology is a critical factor and commercial success relies upon development of the technologies performance. As electrolyzers are relatively mature at current stage this discussion will focus primarily on the potential advances in photovoltaic cells.

##### ***3.1.1 Technology Drivers***

The fundamental difference between electrolysis and PV-electrolysis is the source of the electricity feedstock. The former uses grid electricity whilst the latter obtains electricity from photovoltaic cells. One of the most important reasons for using photovoltaics is the environmentally responsible and sustainable sourcing of electricity feedstock. Recent awareness of environmental issues and a resource constrained future has certainly pushed energy company sentiment in the direction of PV. However for many, unless economical, this alone is not enough to incentivise the use of PV technologies. PV must be an economically competitive technology

which requires continued performance development.

Incremental improvements and learning curves in 1st generation (silicon wafer) solar cells have gradually reduced the costs of PV technology. Although efficient, 1st generation solar cells are expensive because they require thick wafers and vacuum processes for film fabrication.<sup>26</sup> Despite this they are expected to remain the dominant PV technology into 2020 when 2nd generation systems will become prevalent.<sup>27</sup> The 2nd generation (thin film) solar cells are fabricated by deposition of photosensitive materials such as silicon, Cadmium Telluride (CdTe) and Copper-Indium-Diselenide (CIS).<sup>27</sup> Thin films, although at the lower end of the PV technology efficiency spectrum, offer a low-cost option which suits large scale applications where land cost is not significant.<sup>28</sup> The long term future of PV devices may however be in 3rd generation solar cells which seek to combine the advantageous aspects of the 1st and 2nd generation technologies. Promising methods encapsulated in the 3rd generation umbrella term include multi-junction cells, intermediate-band cells, hot carrier cells and spectrum conversion.<sup>29</sup> Taken from literature, Table 3.1 gives a technical summary of PV generations and absorption materials.<sup>30</sup> What is essential here is that vast amounts of potential and opportunity exist for innovation and development in the field of photovoltaics. As investment in R&D continues, the technology and the case for using PV for water splitting will continue to strengthen. Another advantage is of the PV technology is that it supplies DC electricity which is an ideal coupling with the operation need of an electrolyser.<sup>31</sup>

### 3.1.2 Plant Operability

The intermittent nature of solar energy introduces complications to powering electrolysis with PV-electricity. In the field of photovoltaics a capacity utilisation factor (CUF) is defined as the ratio between the annual energy delivered to the energy that would be delivered annually under ideal conditions (Equation 3.1)

$$CUF = \frac{\text{Annual Energy Delivered (kWh)}}{\text{Plant Capacity (kW)} \times 24 \times 364} \quad \text{Equation 3.1}$$

Although clearly affected by day and night, the CUF is also a function of solar irradiance and weather conditions. The CUF of systems where there are generally clear and sunny days, such as

the Nevada desert in the US, have been demonstrated to be around 20%.<sup>32</sup> Practically this means that an electrolyser would only be operational for 1/5th of the year and subject to regular variability in load. While complicated, this is not necessarily prohibitive as one Techno-economic analysis points out.<sup>33</sup> They found that the cost penalties to hydrogen production for CUF of 25% were only 11% higher than for systems with a capacity factor of 95%. Higher costs in the 25% CUF alkaline electrolysers considered in this study were offset largely by factors such as reductions in operation and maintenance (O&M) expense and increases in operation life. However research suggests that PEM electrolysers would be more appropriate for this type of intermittent operation as they have displayed stable performance during dynamic operation.<sup>34</sup>

*Table 3.1 Comparison of PV technology generations and main absorber materials*

Absorber	1st Gen		2nd Gen			3rd Gen	
	Sc-Si	mc-Si	a-Si/ $\mu$ -Si	CdTe	CIGS	DS(S)C	Organic
Maturity of production (%) a	86	89	84	77	80	- d	- d
2010 market share (%) b	39	48	4	7	2	~0	~0
Max cell efficiency (%) c	25.0	20.4	12.3	16.7	19.6	11.0	10.0
Max module efficiency (%) c	21.4	18.2	10.4	12.8	15.7	- d	- d
Commercial efficiency (%)	14	14	6/- d	11	11	- d	- d
Absorber thickness ( $\mu$ m )	180-250		0.2-0.35/1-2	2-5	2-3	~10	0.03-0.2

*Source: Copied from reference 30 with permission from Elsevier.*

a: the maturity of production is obtained by dividing the maximum commercial module efficiency by the maximum laboratory cell efficiency. To the author this represents well the degree of utilization of the potential of the respective technology in terms of commercial production.

b: Share was calculated from annual cell/module shipments in MW.<sup>35</sup>

c: Confirmed terrestrial cell/module efficiencies measured under the global AM1.5 spectrum (1000 W/m<sup>2</sup>) at 25°C (IEC 60904-3: 2008, ASTM G-173-03 global).<sup>36</sup>

d No confirmed terrestrial module efficiencies available.

Table 3.2 Results for PV-electrolysis hydrogen production plant analysis

	PV module efficiency					
	1st Generation			2nd Generation		
	10%	12%	14%	12%	14%	16%
	<b>Cost of hydrogen (\$/kgH<sub>2</sub>)</b>					
20-year PV life	4.89	4.34	3.95	2.78	2.51	2.23
30-year PV life	4.67	4.12	3.75	2.60	2.34	2.12
60-year PV life	-	-	-	1.83	1.68	1.50
	<b>Levelized PV DC Electricity Prices ( ¢/kWh )</b>					
20-year PV life	7.2	6.1	5.3	4.3	3.8	3.3
30-year PV life	6.4	5.4	4.7	4.0	3.5	3.1
60-year PV life	-	-	-	2.6	2.3	2.1

Source: Data obtained from ref. 30

### 3.1.3 Techno-economic Findings

Previous research has attempted to simulate PV-electrolysis operations.<sup>37-42</sup> A gate-to-wheels technoeconomic assessment from 2008 however provides the most comprehensive insight into this technology's future.<sup>33</sup> It argues that because PV module life (approximately 20-30 years) is shorter than Balance of Plant (BOP) life (approximately 60 years), a single PV plant can be constructed across two generations (note these generations are different to the generations of PV technology that are also referred to). After the PV modules from the 1st generation have expired, they can be replaced with PV modules that cover the next 30 years of operation. The capital expenditure for the 2nd generation is much reduced because the BOP components remain from the 1st generation. This study therefore assesses the cost of hydrogen production and distribution across a 1st and 2nd generation facility.

The 1st generation plant assesses the cost of hydrogen production and distribution for 10%, 12% and 14% efficient PV module systems with a 591,780 kg per day capacity. The 2nd generation assumes technological improvement in efficiency over the 30 years of the 1st generation plant and therefore assesses 12%, 14% and 16% efficient PV modules. In addition, the authors posited and investigated that as a relatively new technology thin film PV cells may have operation lifetimes as long as 60 years, an idea that recent research supports.<sup>30</sup> A summary of the results

from the 2008 analysis is shown in Table 3.2. The main finding for the 1st generation plant are that 14% efficient PV modules are required to achieve the DOE's 4-2  $\$/\text{kg}_{\text{H}_2}$  target price. For all efficiencies and across all PV-cell life expectancies the 2nd generation plant met the DOE production cost target and even exceeded it for the sixty-year case. The cost of electricity was again found to be the largest contribution to hydrogen production costs, accounting for over 80% of the total, thus the hypothesis that focusing on the expenditure of solar cell instead of electrolysis cell is reasonable. Because of this, a sensitivity analysis was conducted for both the overall hydrogen cost and PV electricity generation. The base case was taken as a 1st generation plant with 30-year operating life and 12% efficient PV modules. The result of the analysis (Figure 3.1) showed that the cost of hydrogen was most sensitive to PV-electricity cost (black circle) by over a factor of 10 relative to other assessed variables (purple to yellow circles). A 1  $\text{¢}/\text{kWh}$  change in the cost of PV-electricity causes a 0.54  $\$/\text{kg}_{\text{H}_2}$  change in the cost of hydrogen whereas electrolyser O&M expense, the next most sensitive variable, causes a 0.053  $\$/\text{kg}_{\text{H}_2}$  change for a 0.5% change in O&M expense. The cost of PV-electricity was most sensitive to PV module efficiency and insolation level at 0.4  $\text{¢}/\text{kWh}$  for 1% and 0.5 hour ( $21 \text{ W}/\text{m}^2$ ) changes respectively. These results clearly demonstrate how integral the PV technology is to the commercial success of a PV-electrolysis plant. However the study assumed that the sites would receive  $271 \text{ W}/\text{m}^2$  of solar insolation for 6.5 hours daily as a base case which is high relative to the global average. Such requirements for high solar insolation levels therefore implicitly exclude many global regions from using this technology.

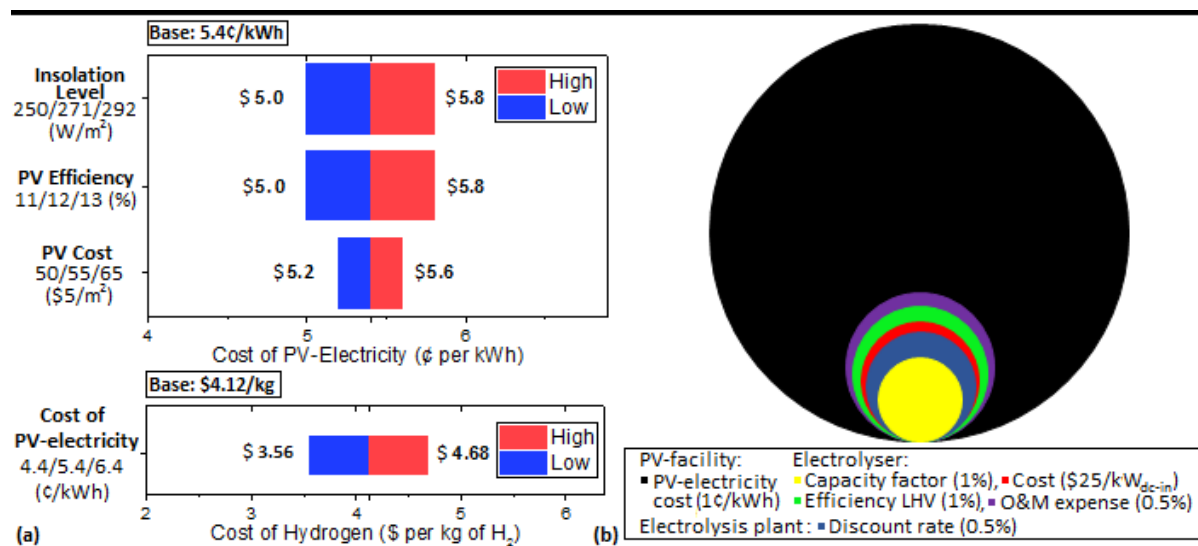


Figure 3.1: (a) Tornado charts produced from results for hydrogen and PV-Electrolysis production cost sensitivity analysis, data obtained from reference 33 and (b) Relative (by area) impact of variables on the cost of hydrogen per unit change in the variable.

However, to provide a contrasting approach to the analysis, the PV and electrolysis systems can also be taken in isolation. Analysis of pure electrolysis from grid electricity also assessed the relationship between electricity price and the impact on the cost of hydrogen.<sup>43</sup> The overall PV-electrolysis system can therefore also be assessed using the grid-electrolysis assessment based on the delivery price of PV-electricity. In the grid-electricity analysis an electricity price of 6.50 2007¢/kWh or lower was required to reach the DOE 4-2 \$/kg<sub>H2</sub> target. The electricity prices in Table 3.2 show that, by this method, the hydrogen cost target would be achieved in all but the most pessimistic case. However contradictory reports expect PV electricity to be significantly more expensive than the 7.2-2.1 ¢/kWh assumed attainable in the PV-electrolysis analysis. The US Energy Information Agency's current projection for the cost of PV-electricity is 9.8-19.3 2013¢/kWh by 2020 depending on site location.<sup>44</sup> Even projections out to 2050 under similar insolation levels show mixed support for prices in the 7.2-2.1 ¢/kWh range.<sup>45-47</sup> Furthermore, Table 3.1 shows that second generation commercial CdTe and CIGS PV modules are already close to the expected performance standards outlined in the PV-electrolysis analysis. Similar research has also looked less favourably on the economics, concluding that PV-electrolysis could be up to 10 times more expensive than grid powered electrolysis.<sup>42, 48</sup> Therefore while the assessment of sensitivities provides valuable system insight, the predicted hydrogen costs are not necessarily reliable.

### ***3.2 Photocatalytic and PEC Water Splitting***

As relatively immature technologies, the basic principles of PEC and photocatalytic water splitting were first demonstrated on a TiO<sub>2</sub> photoanode in 1972.<sup>49</sup> Because of this technical immaturity, demonstrations of photocatalytic systems are still confined to bench scale operations.<sup>50-53</sup> These operations are essential however for exploring reactor materials and providing a basis for future developments.

#### ***3.2.1 Technology Drivers***

Because of its direct utilization of solar energy, photocatalytic water splitting and other PEC processes at suitably high efficiencies have been touted as the 'Holy Grail' of renewable energy sources.<sup>54</sup> In addition to being sustainable, PEC processes offer an end to end solution. In other words, by taking solar energy as the input and directly utilising it to produce hydrogen, there are no intermediate steps that may produce carbon emissions, involve capital expenditure or incur losses.

The delivery pressure of hydrogen is also an important aspect of each system. Delivery pressures of 300 psi (205 bar) can be achieved by compression with suspension systems however are inherent in high pressure PEC cell operation. As future hydrogen storage solutions are likely to include compression, this can potentially save on some costs and is useful for automotive applications.

As with PV-Electrolysis, the separation of oxygen and hydrogen evolution means PEC systems can achieve high product purities. The cogeneration of products in suspension system means a separation stage or novel engineering approaches are required to achieve the required purity. The purity is therefore a function of how rigorous these separations are. The standard (98%) purity has been used for analysis which is still useful for applications in fuel cells.<sup>20</sup>

With a low technology readiness level of 1-2 out of 9, PEC systems are still largely an unknown. Therefore one of the key drivers for this technology is the vast research potential which will undoubtedly lead to improved performance. For example, over the years substantial work has been dedicated to quantifying the realistic efficiencies of PEC devices.<sup>55-58</sup> For tandem photocatalytic systems of interest, the maximum theoretical efficiency is thought to be 40-41%.<sup>59, 60</sup> However considering practical system losses, the maximum obtainable solar-to-hydrogen (STH) efficiency for PEC systems has been calculated as 22.8%.<sup>61</sup> Demonstrated



efficiencies have however thus far fallen short and languish in the low single figures. Stable materials with STH efficiencies of 1-2% have been reported whilst higher efficiencies of 5% have only be obtained for materials with hour timescale stability.<sup>62-65</sup> Photocatalysis and PEC cells are therefore attractive technologies because, as opposed to mature technologies, it is both obvious where the improvements will come from and plausible that they be achieved.

### *3.2.2 Plant Operability*

Because of the reliance on solar energy, utilisation and average daily insolation is an important factor in plant operability. To account for this, systems must be over sized and provide the rated capacity. Achieving high insolation also affects the design of the reactors and panels as the effective capture of light becomes an influential consideration.

Two types of conceptual reactor design and panel arrangement (Figure 3.2) have become popular working models since their use in the most comprehensive economic assessment of the technologies to date.<sup>20</sup> However photo-reactor and panel design are an area of ongoing study.<sup>20,</sup>

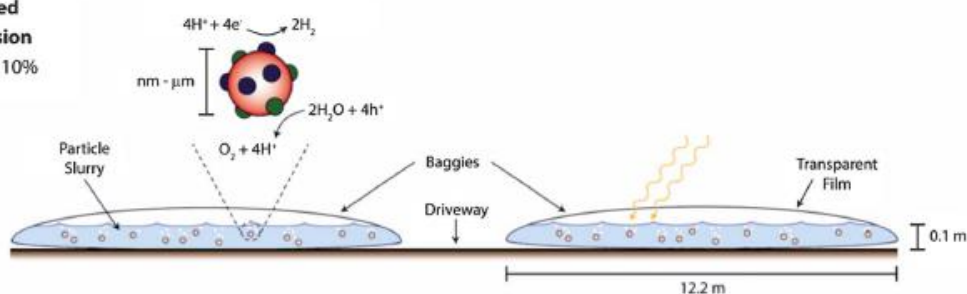
<sup>66</sup> Type 1 reactors are transparent, allowing light to penetrate through, and serve to simply contain the evolved gases and photocatalytic particles suspended with an electrolyte as slurry. The co-generation of gases occurring in Type 1 reactors differentiates Type 2 reactors which instead evolve H<sub>2</sub> and O<sub>2</sub> in separate beds. As well as removing the need for gas separation units, this affords greater potential to optimize the choice of materials for the oxygen evolution reaction (OER) and hydrogen evolution reaction (HER). However this design requires the addition of a redox mediator and porous bridge for transport which introduces additional losses and limitations through media transport rates.<sup>67</sup> Despite being more complex, the Type 2 design avoids the formation and subsequent compression of a combustible hydrogen-oxygen mixture which is a significant safety concern associated with Type 1 reactors. Mitigating risks arising from this hazard may yet incur additional control and gas processing costs not captured in this analysis.

In their construction, Type 3 reactors resemble the solar panels typically associated with the PV technology. These panels are fixed and so face the equator with a pitch that optimises performance across the entire year. The assembly includes the two electrodes which sandwich photoactive layers and operate inside a transparent casing which contains the electrolyte and water. The Type 4 reactor has the same structure as Type 3 reactors however by tracking and concentrating solar radiation, a smaller photocell area is required. Expensive materials with higher efficiency and performance may therefore become economically viable options for these

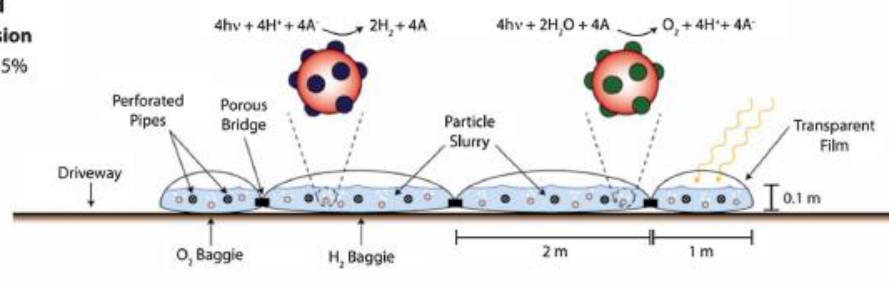
reactor types.

The Type 3 and 4 PEC panel reactors are inherently more complex than the Type 1 and 2 photocatalytic suspension systems. However the panel systems are based on a familiar and proven architecture which has been successfully demonstrated with photovoltaics. Although conceptually simple, until prototypes are developed, operability problems will be difficult to foresee with the suspension systems.

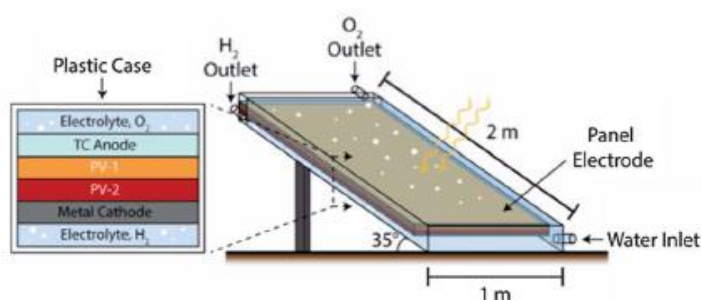
**Type 1: Single Bed Particle Suspension**  
STH Efficiency 10%



**Type 2: Dual Bed Particle Suspension**  
STH Efficiency 5%



**Type 3: Fixed Panel Array**  
STH Efficiency 10%



**Type 4: Tracking Concentrator Array**  
STH Efficiency 15%

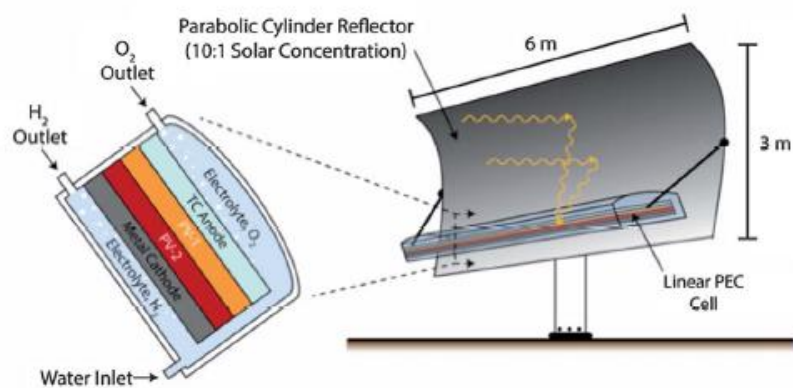


Figure 3.2: Schematic of conceptual reactor types with (a) Type 1 reactor single baggie cross section with particle slurry and (b) Type 2 reactor dual baggie arrangement with separated  $H_2$  and  $O_2$  evolution chambers evolution, (c) Type 3 reactor design showing the encased composite panel oriented toward the sun with buoyant separation of gases, and (d) Type 4 reactor design with an offset parabolic cylinder receiver concentrating light on a linear PEC cell. Reproduced from Ref. 20 with permission from The Royal Society of Chemistry

### 3.2.3 Techno-economic Findings

The foremost research into hydrogen production using PEC devices assessed both the technical and economic feasibility of conceptual centralised plants with a 10,000 kg per day capacity.<sup>20, 68</sup> Results from this study are summarised in Table 3.3 and shall be discussed in the rest of this section.

At 1.63  $\$/\text{kg}_{\text{H}_2}$  Type 1 reactors were found to exceed the DOE's target of 2-4  $\$/\text{kg}_{\text{H}_2}$  and overall provide the most economic arrangement. Type 2 reactors still achieved the target level with a production cost of 3.2  $\$/\text{kg}_{\text{H}_2}$ . While this implies robust economic potential, these figures were calculated by assuming baseline STH efficiencies of 10% and 5% for Type 1 and Type 2 reactors respectively. Such performance from stable materials has not yet been observed and could be many years from discovery if indeed found at all. However the purpose of the paper was to establish whether a favorable economic case existed should technical barriers be overcome. As this has been confirmed, a stronger incentive exists for pursuing research in overcoming such barriers. The only note one may find is the safety issue in Type 1 was not considered here.

The PEC designs were found to have a higher cost of hydrogen production compared to the photocatalytic technology (or suspension system). Type 3 reactors were the most expensive options of all the designs with a cost of 10.36  $\$/\text{kg}_{\text{H}_2}$  whilst Type 4 reactors narrowly missed the 4  $\$/\text{kg}_{\text{H}_2}$  end of the DOE target at 4.05  $\$/\text{kg}_{\text{H}_2}$ . Again these findings are based on efficiency and cost performances which have not yet been observed but are deemed obtainable with sufficient research advancement. Being well outside the target range and with no substantial advantage, the extra cost of the Type 3 reactor cannot be justified. Designs that concentrate solar radiation and continually optimise their position through tracking are therefore the likely choice for future designs. Therefore only Type 4 designs will be considered for further analysis of the PEC system.

*Table 3.3 Results of centralised hydrogen production plant analysis*

Suspension system	Cost of Hydrogen			
	Type 1 Reactor		Type 2 Reactor	
	(2005 \$/kg <sub>H2</sub> )	% of total	( 2005\$/kg <sub>H2</sub> )	% of total
Capital Costs (Direct, Indirect and Land)	0.97	59.5	2.27	70.9
Decommissioning Costs	0.01	0.6	0.02	0.625
Fixed O&M Costs	0.48	29.4	0.8	25
Other Variable Costs	0.17	10.5	0.11	3.44
<b>Total</b>	<b>1.63</b>	<b>100</b>	<b>3.20</b>	<b>100</b>

PEC	Type 3 Reactor		Type 4 Reactor	
	(2005 \$/kg <sub>H2</sub> )	% of total	( 2005\$/kg <sub>H2</sub> )	% of total
	Capital Costs (Direct, Indirect and Land)	8.37	80.8	2.81
Decommissioning Costs	0.07	0.7	0.03	0.7
Fixed O&M Costs	1.82	17.5	1.2	29.7
Other Variable Costs	0.1	1	0.01	0.2
<b>Total</b>	<b>10.36</b>	<b>100</b>	<b>4.05</b>	<b>100</b>

Source: Data obtained from ref. 43

The results show that capital cost were the most significant contribution to overall costs for all technologies. For the photocatalytic Type 1 and Type 2 reactors, the total uninstalled hydrogen production costs were 59.5% and 70.9% respectively (Figure 3.3). For Type 1 reactors high compression costs are caused due to the extra volume of O<sub>2</sub> processed in the product stream. The intrinsic separation of Type 2 reactors mean its compression costs are cheaper although this is more than offset by higher costs in almost every other category. The costs attributed to baggies

are in particular higher for the Type 2 reactors because so many are required which incurs additional fabrication, land and labor costs. The simpler Type 1 reactor coupled with a Pressure Swing Absorption (PSA) unit therefore appears more economical.

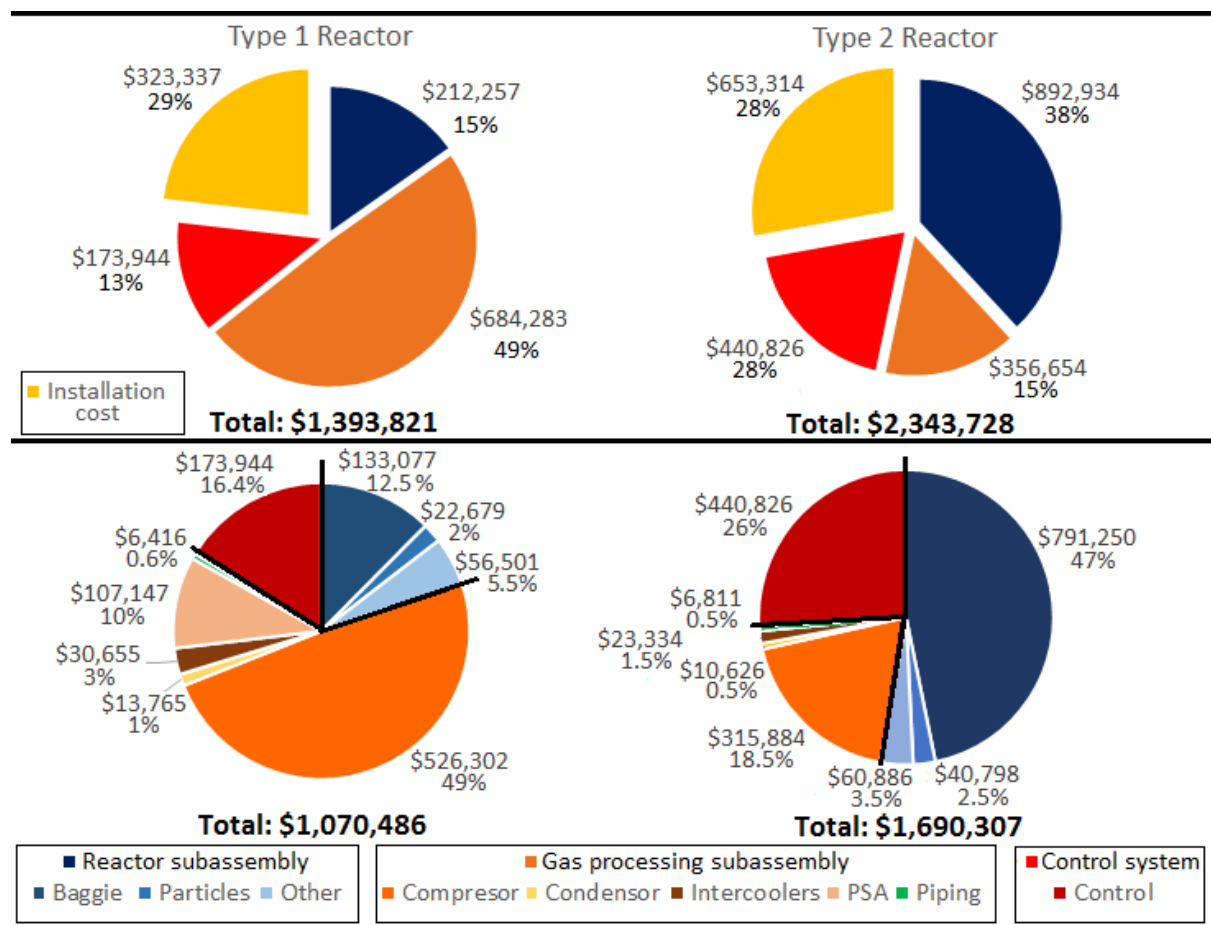


Figure 3.3: Breakdown of capital costs (uninstalled and installed) for Type 1 and Type 2 Reactors; data obtained from references 20 and 68.

Capital costs associated with the panels of the Type 4 PEC system accounted for 80.8% of the uninstalled total with Fixed O&M the other significant contribution at 17.5%. A further breakdown of the costs (Figure 3.4) shows that the tracking and concentration system as well as PEC cells form the majority of these costs. These can be considered key areas of focus for future research in to reducing the costs of these systems. Despite a higher nominal system efficiency of 15%, the uninstalled capital cost and installed total cost of the PEC system is still much higher than the photocatalytic suspension systems. This is almost entirely due to the reactor subassembly which is more costly due to the complex PEC cell design.

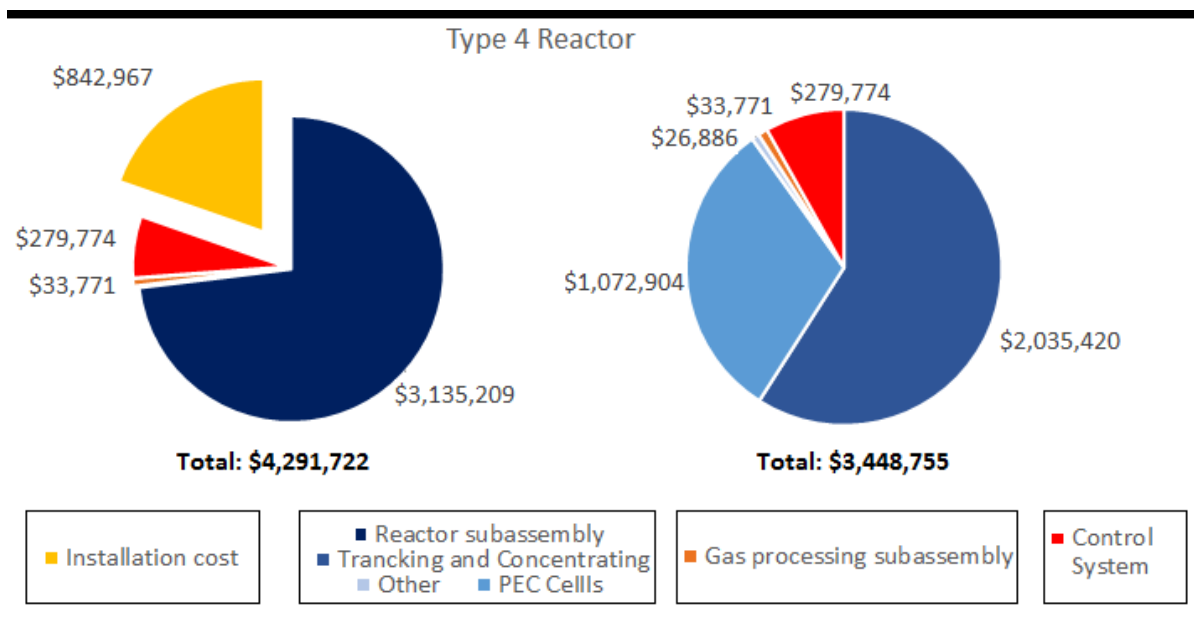


Figure 3.4: Breakdown of capital costs (uninstalled and installed) for Type 4 Reactors; data obtained from references 20 and 68.

To further understand the impact of capital costs and other parameters, a sensitivity analysis was conducted. For the photocatalytic system, the STH efficiency, particle capital costs and system lifetime were all varied over a feasible range with cell cost replacing particle cost for the PEC analysis.

The Tornado Charts for the photocatalytic analysis are shown in Figure 3.5. For both reactor Types the largest effect on hydrogen price was caused by changes to the STH efficiency followed by the particle cost multiplier. While hydrogen from Type 1 reactors remained within the 2-4  $\$/\text{kg}_{\text{H}_2}$  cost target for both high scenarios, the Type 2 reactor was not found to achieve the target for STH efficiencies of 2.5% and particle cost multipliers of 20. As extreme estimates however these findings are far from prohibitive and still result in hydrogen costs lower than many other competing technologies. The effect of the system lifetime was found to have a very limited effect for both the high and low cases. The only low case that caused a significant reduction in hydrogen cost was an STH efficiency of 7.5% in Type 2 reactors where the cost fell by 0.7  $\$/\text{kg}_{\text{H}_2}$ .

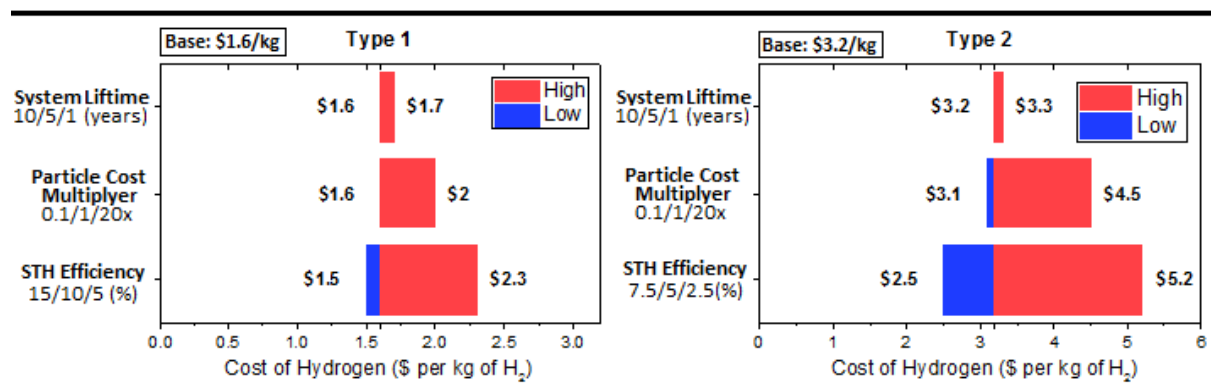


Figure 3.5: Reproduced Tornado Charts for Type 1 and Type 2 reactors showing sensitivity to STH efficiency, particle cost and lifetime. Figure modified and reproduced from Ref. 20 with permission from The Royal Society of Chemistry

The results of a similar analysis for the PEC system are shown in Figure 3.6. Again the STH efficiency has the greatest influence on the overall cost of hydrogen production with a range of 2.7-5.6  $\$/\text{kg}_{\text{H}_2}$  for the 25% and 10% STH efficiency respectively. Reducing the hydrogen cost by 1.3  $\$/\text{kg}_{\text{H}_2}$ , a 25% STH efficiency demonstrated the greatest benefit of any variable across all the technologies. This highlights the importance of the variable to the overall credibility of the system. The sensitivity to system lifetime and cell cost is relatively contained with a 0.1 and 0.3  $\$/\text{kg}_{\text{H}_2}$  benefit respectively in the low case and a 0.5  $\$/\text{kg}_{\text{H}_2}$  penalty for both in the high case. Although the sensitivities technically bring the cost above the target price, the analysis still demonstrates that PEC cells are an economically viable technology. This credibility warrants further research where STH efficiency is a clear priority.

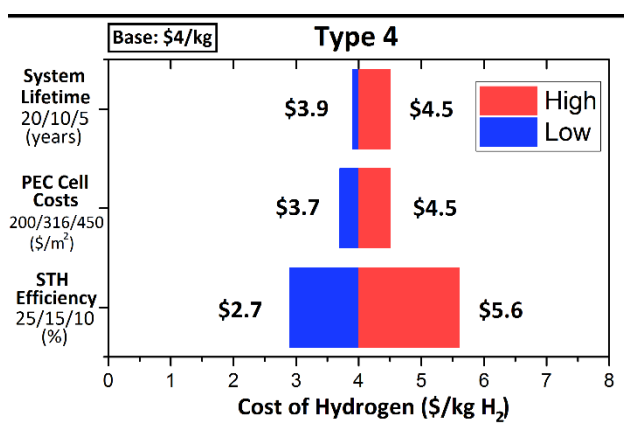


Figure 3.6: Reproduced Tornado Charts for Type 4 reactors showing sensitivity to STH efficiency, PEC cell cost and system lifetime. Figure modified and reproduced from Ref. 20 with permission from The Royal Society of Chemistry

Unlike PV-electrolysis, this study did not investigate the effect of solar insolation for either



technology. An average insolation level of  $219 \text{ W/m}^2$  was assumed which, is close to the global average, opens up more potential regions. Future work analysing the impact of solar insolation on this technologies feasibility would be welcome.

Overall the economic case for centralized hydrogen production via photocatalysis is the more robust of the two technologies. The photocatalysis systems appear able to consistently produce hydrogen under the target price for even the high cases. However, safely processing the combustible mixture in Type 1 reactors and suitable redox mediators and bridge materials in Type 2 reactors remain challenges for photocatalytic systems. The realisation of the particle-bag architecture also remains an unknown which may be significant for the future of the photocatalytic systems. The analysis also provides an economic endorsement for PEC systems which, with sufficient development, will also price competitively. Caveats to both systems are that the envisaged technical performance targets, such as STH efficiency, must be reached. However many of the performance parameters used in the analysis still require substantial research efforts for these systems to be realised. As such the next section will investigate some of the PEC materials with the potential to achieve the required activity and stability. If successful, reactor 4 will be applied.

## 4. Material development for PEC water splitting

### 4.1 Photoanode materials

There are many candidates for photoanode materials and so this section will primarily focus on summarizing the low cost and efficient ones as well as strategies to improve their performance.

(1)  $\text{BiVO}_4$  (BVO) is an n-type semiconductor consisting of relatively inexpensive and abundant elements. It has a direct band gap of 2.4 eV with a conduction band near 0 V vs RHE and valence band at ca. 2.4eV vs RHE. Therefore, photo-generated holes from  $\text{BiVO}_4$  have sufficient overpotential to oxidise water. However, an external bias is required to conduct water reduction reactions.<sup>69-71</sup> Theoretically, the maximum photocurrent and STH efficiency of BVO are  $7.4\text{mA}/\text{cm}^2$  and 9.1% respectively.<sup>70, 72</sup> The efficiency of BVO is limited by: (1) fast charge carriers recombination due to short electron diffusion length of BVO (only 10nm)<sup>73, 74</sup> and (2) poor surface water oxidation kinetics. Electron diffusion length can be significantly increased up to  $\sim 300\text{nm}$  by doping BVO with Mo and W with a diffusion coefficient of  $1.5 \times 10^{-7} \text{cm}^2/\text{s}$ <sup>71, 72, 75, 76</sup> and poor surface kinetics can be modified by surface oxygen evolution co-catalysts such as Co-Pi.<sup>73, 77</sup> To date, Zhong et al has reported a near zero recombination loss by using W-doped BVO photoanode with Co-Pi modification.<sup>73</sup> Recently, for a single BVO photoanode, a benchmark photocurrent of  $2.73\text{mA}/\text{cm}^2$  at 0.6V (vs RHE) was achieved on the nanoporous BVO photoanode with a  $\text{FeOOH}/\text{NiOOH}$  dual layer as the OER catalyst.<sup>78</sup> By assembling a tandem cell with silicon, the benchmark efficiency of 4.6% was reached using a BVO based photoanode.<sup>79</sup>

(2)  $\text{CdS}$ . Theoretically, overall water splitting under visible light irradiation can be achieved by using  $\text{CdS}$  due to the small band gap (2.4eV) as well as a conduction and valence band that straddle the redox potential for pure water splitting.<sup>80</sup> Although it has a long charge carrier diffusion length (up to the micrometer scale), slow water oxidation kinetics leads to photogenerated holes accumulation at the surface, and thus anodic photocorrosion occurs. Therefore, a stabilization strategy must be applied on similar group II-VI semiconductor materials (e.g.  $\text{CdS}$ ,  $\text{CdTe}$ ,  $\text{CdSe}$ ,  $\text{ZnTe}$ ) for solar-driven PEC water splitting processes. One strategy is to use sacrificial hole scavengers such as  $\text{EDTA}$ ,<sup>81</sup>  $\text{Fe}(\text{CN})_6^{4-}$ ,<sup>82</sup>  $\text{S}^{2-}$ ,<sup>83</sup> and  $\text{SO}_3^{2-}$ ,<sup>83</sup> that produce hydrogen. However, in order for the water oxidation reaction to occur on the  $\text{CdS}$

photoanode, hole scavengers cannot be added to the system. Therefore another strategy is used whereby an insulation layer is added to prevent from photocorrosion. Recently, Lewis et al demonstrated that n type CdTe photoanodes could be stabilized when 140 nm thick amorphous TiO<sub>2</sub> by atomic-layer deposition was used together with a thin overlayer of a Ni-oxide based oxygen-evolution electrocatalyst.<sup>84</sup> Borse et al reported CdS photoanodes modified with TiO<sub>2</sub> nanoparticles via thioglycerol as an organic linker for long-term hydrogen production,<sup>85</sup> and that CdS photoanodes could also be modified by nanoniobia for an efficient and stable PEC cell.<sup>86</sup> The n-type cadmium telluride photoanode could also be protected by sputtering transparent catalytic nickel oxide (NiO) on the surface which serves not only as a protection layer, but also as an efficient oxygen evolution co-catalyst.<sup>71</sup> With respect to the efficiency, a recent study has shown that a low hole transfer rate was an efficiency-limiting factor in a CdS-based heterostructure.<sup>70</sup>

(3) *III-V* compounds. The *III-V* compounds semiconductors such as GaAs and InP, and quaternary alloys have great potential to photoelectrodes in PEC cells. In general, *III-V* semiconductors possess several characteristics which make them advantageous for PEC water splitting: (1) Their band gaps are narrow ( 1.42 eV for GaAs and 1.35 eV for InP) which is ideal for light absorption and as such near-optimal absorptivity of the solar spectrum can be achieved,<sup>87</sup> (2) They exhibit extraordinary charge carrier mobility, for example, GaAs has an electron mobility of up to 9200 cm<sup>2</sup> V<sup>-1</sup> S<sup>-1</sup>, and hole mobility up to 400 cm<sup>2</sup> V<sup>-1</sup> S<sup>-1</sup>.<sup>74</sup> Turner et al fabricated a monolithic PV/PEC device for hydrogen production via water splitting with an impressive STH efficiency of 12.6% by using a tandem cell consisting of a p/n GaAs bottom cell connected to a GaInP<sub>2</sub> top cell through a tunnel diode interconnect.<sup>88</sup> Although when compared to metal oxides such as TiO<sub>2</sub>, Fe<sub>2</sub>O<sub>3</sub>, TiO<sub>2</sub>, high photocurrent and STH efficiency can be achieved by *III-V* (Figure 4.1), the instability and high cost limit the semiconductor applications.<sup>89</sup> Recently, Lewis demonstrated that GaAs and GaP could be stabilized against photoanodic corrosion or dissolution by the use of a conformal ALD deposited TiO<sub>2</sub> layer in conjunction with Nickel oxide/hydroxide as an electrocatalyst.<sup>69, 84, 89</sup> The group also reported that GaAs, GaP and InP could be protected by a multifunction layer of NiOx.<sup>90, 91</sup> The NiOx acted as not only a protection layer, but also an efficient oxygen evolution cocatalyst.

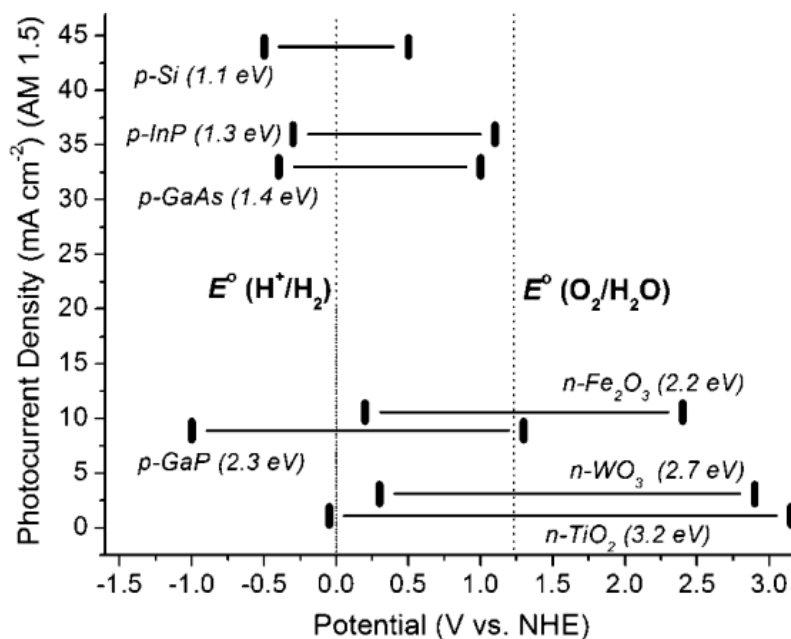


Figure 4.1: The band gap position of various semiconductors and their theoretical photocurrent. Reprinted with permission from reference 25. Copyright (2010) American Chemical Society.

#### 4.2 Photocathode materials

P type materials such as cuprous oxide ( $\text{Cu}_2\text{O}$ ),<sup>92</sup> Si,<sup>93</sup> and  $\text{SiC}$ <sup>94</sup> with a conduction band more negative than the redox potential of ( $\text{H}^+/\text{H}_2$ ) are considered good candidates for a photocathode. However, due to cathodic photocorrosion in electrolyte, their application as a photocathode is still limited.<sup>95, 96</sup>

Cuprous oxide ( $\text{Cu}_2\text{O}$ ) is a p-type semiconductor with a direct band-gap of  $\sim 2$  eV and suitable conduction band position that enables visible light absorption and hydrogen evolution.<sup>76, 97, 98</sup> A theoretical photocurrent of  $\sim 15$   $\text{mA cm}^{-2}$  and 18% STH efficiency can be achieved by a  $\text{Cu}_2\text{O}$  photocathode under AM 1.5 light based on its bandgap.<sup>99</sup> Furthermore, due to the low cost of  $\text{Cu}_2\text{O}$ , large-scale fabrication of the photoelectrode is also attractive. However, the major drawbacks of  $\text{Cu}_2\text{O}$  in solar hydrogen production are the low practical STH efficiency due to the fast electron-hole recombination and poor stability because the redox potentials for the reduction and oxidation of monovalent copper oxide lie within the band-gap.<sup>95, 98</sup> To address these issues, several strategies have been applied on  $\text{Cu}_2\text{O}$  photocathodes including (1) combining with other n-type semiconductors with more positive conduction bands, such as  $\text{TiO}_2$ ,<sup>100</sup>  $\text{ZnO}$ ,<sup>101</sup>  $\text{WO}_3$ ,<sup>102</sup> RGO<sup>103</sup> etc, and (2) forming a n-p junction to allow fast transfer of photo-induced

electrons from  $\text{Cu}_2\text{O}$  to the conduction band of a n-type semiconductor.<sup>104</sup> This improves both the efficiency and stability. In addition, deposition of a thin protection layer on  $\text{Cu}_2\text{O}$  also works. The protection layer could be a thin layer of carbon or  $\text{NiOx}$ . Recently, Grätzel *et al.* reported a  $\text{Cu}_2\text{O}/\text{ZnO}/\text{Al}_2\text{O}_3/\text{TiO}_2/\text{Pt}$  electrode, resulting in a benchmark photocurrent of  $-7.6 \text{ mA cm}^{-2}$  at 0 V vs. RHE with improved stability due to the protective nature of  $\text{TiO}_2$  and high conductivity of  $\text{ZnO}/\text{Al}_2\text{O}_3$  (AZO).<sup>105</sup> The group also designed a similar device consisting of a  $\text{Cu}_2\text{O}/\text{n-AZO}/\text{TiO}_2/\text{MoS}_{2+x}$  heterojunction photocathode that exhibited improved photocurrent and stability in harsh acidic environments ( $-5.7 \text{ mA cm}^{-2}$  at 0 V vs. RHE at pH 1.0).<sup>106</sup> Very recently, a  $\text{Cu}_2\text{O}$ -based photocathode of  $-6.3 \text{ mA cm}^{-2}$  at 0 V vs. RHE in 1 M KOH electrolyte was achieved by coupling surface protected  $\text{Cu}_2\text{O}$  with a  $\text{MoS}_2$  HER catalyst.<sup>107</sup> This appears to be the first report of  $\text{MoS}_2$  as a highly active hydrogen evolution catalyst in basic medium.  $\text{MoS}_2$  thus demonstrates significant potential as an earth-abundant HER catalyst alternative to platinum for water splitting in alkaline conditions.

Silicon has a small band gap of 1.1 eV, which is nearly ideal for use in a dual band gap p/n –PEC water splitting configurations (tandem PEC water-splitting devices). A few reviews have summarised that p-Si photocathode combined with co-catalysts can be used to produce  $\text{H}_2$  efficiently.<sup>93</sup> STH efficiency as high as 6% under monochromatic 633 nm illumination has been achieved by a p-Si photocathode embedded with Pt nanoparticles. It is well known that silicon is not stable in aqueous solution under illumination. Therefore several groups have deposited a corrosion-resistant protective layer on top of p-type and n-type silicon which acts as a photocathode and photoanode for  $\text{H}_2$  and  $\text{O}_2$  production, respectively. Ji *et al.* demonstrated a silicon-based photocathode for water reduction with an epitaxial  $\text{SrTO}_3$  protection layer and a mesh-like Ti/Pt nanostructured cocatalyst. This resulted in a long term (35h) performance in 0.5M  $\text{H}_2\text{SO}_4$  with an applied bias photon-to-current efficiency of 4.9%. Very recently, stabilization of silicon photoanodes in alkaline condition has attracted more attention. Si photoanodes have been stabilized by several novel strategies including: (i) deposition of catalytic transition-metal coatings (e.g.  $\text{CoOx}$ <sup>108</sup> and  $\text{NiOx}$ <sup>109</sup>), (ii) deposition of ultra-thin metal films (e.g. Ni) on an oxidised Si surface,<sup>110 111</sup> and (iii) ALD deposition of a thin amorphous  $\text{TiO}_2$  layer between Si and a surface oxygen co-catalyst such as an  $\text{IrO}_2$  layer<sup>112</sup> or islands of Ni oxide electrocatalyst.<sup>89, 113</sup> Tandem PEC water-splitting devices based on multijunction of silicon (p/n Si-PEC) have large potential as they are able to achieve solar-driven water splitting without a

bias. In addition, n-type semiconductors such as  $\text{BiVO}_4$ ,<sup>79, 114</sup>  $\text{WO}_3$ ,<sup>114</sup>  $\text{Fe}_2\text{O}_3$ ,<sup>115</sup>  $\text{ZnO}$ ,<sup>116</sup> can be coupled with the surface to protect the silicon cell and achieve efficient photocatalytic water oxidation.

### **4.3 Co-catalyst selection**

Noble metal-based catalysts such as  $\text{IrO}_2$  and  $\text{RuO}_2$  are among the best OECs, but prohibitively expensive.<sup>117 118</sup> In recent years, abundant 1st row transition metal oxides have been demonstrated to be excellent OECs.<sup>119</sup> For PEC water oxidation co-catalysts, most of these metal oxides are  $\text{CoOx}$  or  $\text{NiOx}$ .<sup>120</sup>

For OECs coupled with a photoanode in a PEC cell, cobalt oxide prepared by electrodeposition has emerged as an efficient water oxidation catalyst - able to operate under neutral conditions.<sup>121</sup> Nocera and co-workers prepared cobalt oxide films from phosphate buffer (Co-Pi)<sup>122</sup> or borate buffer (CoBi)<sup>123</sup> solution at potential above 1.1V vs NHE.<sup>124 120</sup> The obtained film was amorphous and contained substantial amounts of anions from the phosphate or borate buffer solution. The buffer solution was essential for the deposition of highly active films as well as maintaining their stability. However, the films were unstable in the electrolyte in the absence of an applied bias. The mechanism of these films for water oxidation has been investigated by in situ XAS, which demonstrated that  $\text{O}_2$  evolution was accompanied by an increase in the intensity of a Co (IV) EPR signal.<sup>125</sup>

Nickel (Ni) is another earth-abundant element from the first transition metal row. Nickel based OECs have been widely used on electrochemical and PEC water splitting. Dai and co-workers demonstrated that a thin layer of Ni metal could be used as an OEC and passivation layer for silicon photoanodes.<sup>110</sup> Nickel oxide ( $\text{NiO}_x$ ) prepared by electrodeposition,<sup>126</sup> sputtering,<sup>90</sup> and sol-gel process<sup>127</sup> has been intensely studied in literature. However, most of the prepared  $\text{NiOx}$  films were converted to either  $\text{Ni(OH)}_2$ <sup>128</sup> or  $\text{NiOOH}$  during the water oxidation reaction in an alkaline electrolyte (KOH solution). Yan and co-workers found that the highly nanostructured  $\alpha\text{-Ni(OH)}_2$  nanocrystals could be a remarkably active and stable OER catalyst in alkaline media. They achieved a current density of  $10\text{mA/cm}^2$  at a small overpotential of 0.331V and a small Tafel slope of 42mV/decade. It was also found that the stability performance of  $\alpha\text{-Ni(OH)}_2$  nanocrystals was much better than precious  $\text{RuO}_2$ .<sup>129</sup> Naldoni et al demonstrated that a thin layer

of photodeposited amorphous NiOOH coupled onto a hematite ( $\alpha$ -Fe<sub>2</sub>O<sub>3</sub>) photoanode could reduce the overpotential (onset potential shift by 150mV) and increase the photocurrent by about 50% at 1.23V vs RHE.<sup>21</sup> Nocera and his co-workers also reported Nickel borate (Ni-B<sub>i</sub>), prepared either by electrodeposition or photoelectrodeposition in the presence of nickel precursor (nickel nitrate or nickel chloride) and borate buffer,<sup>130</sup> have been widely used to enhance the efficiency of Fe<sub>2</sub>O<sub>3</sub>,<sup>131</sup> ZnO,<sup>132, 133</sup> WO<sub>3</sub>,<sup>134</sup> and BiVO<sub>4</sub>.<sup>135</sup> On the other hand, catalysts such as Ni-B<sub>i</sub> could undergo self-healing in proper electrolyte (potassium borate solution), which enabled water oxidation over a prolonged period.<sup>136, 137</sup>

FeOOH has been coupled with various semiconductor materials to act as a photoanode for efficient water oxidation. Mullins and co-workers deposited  $\alpha$ -FeOOH onto Si triple junction solar cells with a photovoltaic efficiency of 6.8%. The obtained photoanode ( $\alpha$ -FeOOH/Si) achieved a STH efficiency of 4.3% at 0 V vs RHE in a three-electrode system with 4h life time.<sup>138</sup> Ye et al reported that FeOOH could be loaded onto hematite photoanodes by photoelectrodeposition. The photocurrent of obtained FeOOH/ Fe<sub>2</sub>O<sub>3</sub> films increased nearly four folds at 0.43V (vs RHE) and the onset potential exhibited a cathodic shift by 140mV compared to a bare hematite photoanode. In addition, long term stability (70h) was achieved by Fe<sub>2</sub>O<sub>3</sub>/FeOOH photoanodes.<sup>119</sup>

Incorporating Fe into the nickel hydroxide induced the formation of NiFe layered double hydroxide (NiFe-LDH).<sup>139, 140</sup> The NiFe-LDH OEC exhibited higher electrocatalytic activity for oxygen evolution than either NiOOH or FeOOH catalyst.<sup>141</sup> Ni-Fe LDH could be prepared by a hydrothermal or photoelectrodeposition method onto a semiconductor material. Schmuki and co-workers introduced a NiFe-LDH co-catalyst onto a Ta<sub>3</sub>N<sub>5</sub> electrode by the hydrothermal method. The obtained NiFe-LDH/ Ta<sub>3</sub>N<sub>5</sub> electrode exhibited photocurrent of 6.3mA/cm<sup>2</sup> at 1.23 V<sub>RHE</sub> in 1M KOH and improved the stability over the test period compared to bare Ta<sub>3</sub>N<sub>5</sub>.<sup>140</sup> Domen demonstrated that nanoworm BiVO<sub>4</sub> with Ni-Fe-LDH modification, prepared by photoelectrodeposition, exhibited high STH efficiency (2.25%) and long term durability (10h) in a 1 M potassium borate electrolyte (pH = 9.3) under AM1.5 one sun illumination.<sup>142</sup>

For water reduction, Noble metals such as platinum (Pt) are frequently used due to their low overpotential and strong corrosion resistance.<sup>143</sup> However, efficient non-precious hydrogen evolution catalysts including metal sulfides, metal selenides, metal carbides, metal nitrides, metal phosphides, and heteroatom-doped nanocarbons are essential for economical H<sub>2</sub> production.<sup>144</sup>

## 5. Conclusion

In summary, the techno-economic assessment of three methods of producing hydrogen through splitting water has been carried out. For PV-electrolysis plants, the cost of electricity feedstock was found to have the most influence on the overall cost of producing hydrogen. Improving the efficiency of electrolyzers can reduce this burden somewhat but developing PV technology play a key role to provide a cheap electricity feedstock. Photocatalysis and PEC cells are still technically immature but indicate promise for the future. Current challenges involve discovering new materials that can prevent electron-hole recombination and utilise a higher proportion of the solar spectrum to increase STH efficiency which dominates the overall costs in the two technologies. Once this is achieved it is envisaged that capital costs will become a significant, but not prohibitive, expense to reduce.

Hydrogen production from photocatalysis provided the most positive economic case with both Type 1 and Type 2 reactors producing hydrogen at 1.6  $\$/\text{kg}_{\text{H}_2}$  and 3.20  $\$/\text{kg}_{\text{H}_2}$ , respectively. Only the Type 4 reactor that utilises PEC technology was deemed sufficiently competitive, producing hydrogen at 4.05  $\$/\text{kg}_{\text{H}_2}$ . Although more expensive, the inherent separation of gases and greater certainty of architecture means PEC systems provide a more well-rounded and holistic solution. In addition, sufficient advancements in the STH efficiency of PEC devices can potentially reduce the cost to 2.7  $\$/\text{kg}_{\text{H}_2}$ . This would bring the economic performance within the US DOE target and in line with the photocatalytic technology. For these reasons, although both remain interesting prospects for the future, PEC system are favored. The further analysis on the different components in a PEC cell underlines the group III-V compounds have a strong potential to meet the target of high STH efficiency, together with an appropriate cocatalyst which also works as a protection layer from photocorrosion. However other photoelectrodes (including metal oxides, sulphides and so on) are not ruled out at this stage. In total, a highly efficient PEC device with an affordable cost and stability is the most important in the solar driven water splitting field.



## References

1. N. S. Lewis and D. G. Nocera, *Proceedings of the National Academy of Sciences*, 2006, **103**, 15729-15735.
2. J. Barber, *Chemical Society Reviews*, 2009, **38**, 185-196.
3. R. van de Krol, in *Photoelectrochemical Hydrogen Production*, eds. R. van de Krol and M. Grätzel, Springer US, Boston, MA, 2012, vol. 102, ch. 2, pp. 13-67.
4. J. O. M. Bockris, B. E. Conway and E. Yeager, *Comprehensive treatise of electrochemistry*, Plenum Press, New York, 1981.
5. A. Brinner, H. Bussmann, W. Hug and W. Seeger, *International Journal of Hydrogen Energy*, 1992, **17**, 187-197.
6. P. A. Lehman and C. E. Chamberlin, *International Journal of Hydrogen Energy*, 1991, **16**, 349-352.
7. S. Galli, *International Journal of Hydrogen Energy*, 1997, **22**, 453-458.
8. A. Garcia-Conde and F. Rosa, *International Journal of Hydrogen Energy*, 1993, **18**, 995-1000.
9. M. M. Rashid, M. K. Al Mesfer, H. Naseem and M. Danish, *International Journal of Engineering and Advanced Technology*, 2015, **4**, 80-93.
10. D. Shapiro, J. Duffy, M. Kimble and M. Pien, *Solar Energy*, 2005, **79**, 544-550.
11. B. Paul and J. Andrews, *International Journal of Hydrogen Energy*, 2008, **33**, 490-498.
12. O. Atlam, *International Journal of Hydrogen Energy*, 2009, **34**, 6589-6595.
13. R. E. Clarke, S. Giddey, F. T. Ciacchi, S. P. S. Badwal, B. Paul and J. Andrews, *International Journal of Hydrogen Energy*, 2009, **34**, 2531-2542.
14. H. Steeb, A. Mehrmann, W. Seeger and W. Schnurnberger, *International Journal of Hydrogen Energy*, 1985, **10**, 353-358.
15. F. Petrakopoulou, J. Sanz-Bermejo, J. Dufour and M. Romero, *Energy*, 2016, **94**, 304-315.
16. S. R. Wenham, M. A. Green, M. E. Watt and R. Corksih, *Applied Photovoltaics*, Earthscan, 2009.
17. T. Markvart, *Solar Electricity*, John Wiley & Sons, 2000.
18. S. C. W. Krauter, *Solar Electric Power Generation - Photovoltaic Energy Systems: Modeling of Optical and Thermal Performance, Electrical Yield, Energy Balance, Effect on Reduction of Greenhouse Gas Emissions*, Springer Science & Business Media, 2007.
19. A. Luque and S. Hegedus, *Handbook of Photovoltaic Science and Engineering*, John Wiley & Sons, 2011.
20. B. a. Pinaud, J. D. Benck, L. C. Seitz, A. J. Forman, Z. Chen, T. G. Deutsch, B. D. James, K. N. Baum, G. N. Baum, S. Ardo, H. Wang, E. Miller and T. F. Jaramillo, *Energy & Environmental Science*, 2013, **6**, 1983-2002.
21. D. J. Martin, K. Qiu, S. A. Shevlin, A. D. Handoko, X. Chen, Z. Guo and J. Tang, *Angewandte Chemie International Edition*, 2014, **53**, 9240-9245.
22. C. Jiang, K. Y. Lee, C. M. Parlett, M. K. Bayazit, C. C. Lau, Q. Ruan, S. J. Moniz, A. F. Lee and J. Tang, *Applied Catalysis A: General*, 2015, DOI:10.1016/j.apcata.2015.1012.1004.
23. D. J. Martin, N. Umezawa, X. Chen, J. Ye and J. Tang, *Energy & Environmental Science*, 2013, **6**, 3380-3386.
24. A. Kudo and Y. Miseki, *Chem Soc Rev*, 2009, **38**, 253-278.

25. M. G. Walter, E. L. Warren, J. R. McKone, S. W. Boettcher, Q. Mi, E. a. Santori and N. S. Lewis, *Chemical Reviews*, 2010, **110**, 6446-6473.
26. Q. Wang, Y. Xie, F. Soltani-Kordshuli and M. Eslamian, *Renewable and Sustainable Energy Reviews*, 2016, **56**, 347-361.
27. N. Tanaka, *Energy technology perspective: Scenario and strategies to 2050*, Paris, 2008.
28. N. Tanaka, *Energy Technology Perspectives: Scenarios and Strategies To 2050*, Paris, 2010.
29. G. F. Brown and J. Wu, *Laser & Photonics Reviews*, 2009, **3**, 394-405.
30. S. Abermann, *Solar Energy*, 2013, **94**, 37-70.
31. G. Conibeer and B. Richards, *International Journal of Hydrogen Energy*, 2007, **32**, 2703-2711.
32. X. Liu, S. K. Hoekman, C. Robbins and P. Ross, *Solar Energy*, 2015, **119**, 561-572.
33. J. Mason and K. Zweibel, in *Solar Hydrogen Generation: Toward a Renewable Energy Future*, eds. R. McConnell and K. Rajeshwar, Springer, 2008, vol. 1, pp. 273-313.
34. P. Millet and S. Grigoriev, *Renewable Hydrogen Technologies: Production, Purification, Storage, Applications and Safety*, 2013, 19-41.
35. K. Ardani and R. Margolis, *2010 Solar Technologies Market Report*, U.S. Department of Energy, 2011.
36. M. A. Green, K. Emery, Y. Hishikawa, W. Warta and E. D. Dunlop, *Progress in Photovoltaics: Research and Applications*, 2012, **20**, 12-20.
37. A. Paola, Z. Fabrizio and O. Fabio, *International Journal of Hydrogen Energy*, 2011, **36**, 1371-1381.
38. D. Bezmalinović, F. Barbir and I. Tolj, *International Journal of Hydrogen Energy*, 2013, **38**, 417-425.
39. F. Saeed, A. Al-ghandoor and Y. Al-husban, presented in part at the SET2011, 10th International Conference on Sustainable Energy Technologies, 2011.
40. A. Balabel, M. S. Zaky and I. Sakr, *Arabian Journal for Science and Engineering*, 2014, **39**, 4211-4220.
41. T. L. Gibson and N. A. Kelly, *International Journal of Hydrogen Energy*, 2010, **35**, 900-911.
42. F. Muller-Langer, E. Tzimas, M. Kaltschmidt and S. Peteves, *International Journal of Hydrogen Energy*, 2007, **32**, 3797-3810.
43. B. James, W. Colella, M. Jennie, G. Saur and T. Ramsden, *PEM Electrolysis H2A Production Case Study*, 2013.
44. EIA, Levelized Cost and Levelized Avoided Cost of New Generation Resources in the Annual Energy Outlook 2015, [https://www.eia.gov/forecasts/aeo/electricity\\_generation.cfm](https://www.eia.gov/forecasts/aeo/electricity_generation.cfm), Accessed March, 2016.
45. C. Parrado, A. Girard, F. Simon and E. Fuentealba, *Energy*, 2016, **94**, 422-430.
46. R. Tidball, J. Bluestein, N. Rodriguez and S. Knoke, *Cost and performance assumptions for modeling electricity generation technologies*, National Renewable Energy Laboratory 2010.
47. A. S. Mundada, K. K. Shah and J. M. Pearce, *Renewable and Sustainable Energy Reviews*, 2016, **57**, 692-703.
48. C. Acar and I. Dincer, *International Journal of Hydrogen Energy*, 2014, **39**, 1-12.
49. A. Fujishima and K. Honda, *Nature*, 1972, **238**, 37-38.
50. D. Jing, L. Guo, L. Zhao, X. Zhang, H. Liu, M. Li, S. Shen, G. Liu, X. Hu and X. Zhang,

- International Journal of Hydrogen Energy*, 2010, **35**, 7087-7097.
51. D. Spasiano, R. Marotta, S. Malato, P. Fernandez-Ibañez and I. Di Somma, *Applied Catalysis B: Environmental*, 2015, **170-171**, 90-123.
  52. E. Baniasadi, I. Dincer and G. F. Naterer, *Chemical Engineering Journal*, 2012, **213**, 330-337.
  53. K. Villa, X. Domènech, S. Malato, M. I. Maldonado and J. Peral, *International Journal of Hydrogen Energy*, 2013, **38**, 12718-12724.
  54. A. J. Bard and M. A. Fox, *Accounts of Chemical Research*, 1995, **28**, 141-145.
  55. M. F. Weber and M. J. Dignam, *International Journal of Hydrogen Energy*, 1986, **11**, 225-232.
  56. M. F. Weber and M. J. Dignam, *Journal of The Electrochemical Society*, 1984, **131**, 1258.
  57. J. R. Bolton, S. J. Strickler and J. S. Connolly, *Nature*, 1985, **316**, 495-500.
  58. R. E. Rocheleau and E. Miller, *International Journal of Hydrogen Energy*, 1997, **22**, 771-782.
  59. R. T. Ross and T. L. Hsiao, *Journal of Applied Physics*, 1977, **48**, 4783.
  60. M. C. Hanna and A. J. Nozik, *Journal of Applied Physics*, 2006, **100**, 74510.
  61. L. C. Seitz, Z. Chen, A. J. Forman, B. A. Pinaud, J. D. Benck and T. F. Jaramillo, *ChemSusChem*, 2014, **7**, 1372-1385.
  62. D. M. Fabian, S. Hu, N. Singh, F. A. Houle, T. Hisatomi, K. Domen, F. Osterloh and S. Ardo, *Energy & Environmental Science*, 2015, **8**, 2825-2850.
  63. Q. Wang, T. Hisatomi, Q. Jia, H. Tokudome, M. Zhong, C. Wang, Z. Pan, T. Takata, M. Nakabayashi, N. Shibata, Y. Li, I. D. Sharp, A. Kudo, T. Yamada and K. Domen, *Nature Materials*, 2016, Doi:10.1038/nmat4589.
  64. L. Liao, Q. Zhang, Z. Su, Z. Zhao, Y. Wang, Y. Li, X. Lu, D. Wei, G. Feng, Q. Yu, X. Cai, J. Zhao, Z. Ren, H. Fang, F. Robles-Hernandez, S. Baldelli and J. Bao, *Nature Nanotechnology*, 2013, **9**, 69-73.
  65. J. Liu, Y. Liu, N. Liu, Y. Han, X. Zhang, H. Huang, Y. Lifshitz, S.-t. Lee, J. Zhong and Z. Kang, *Science*, 2015, **347**, 1-6.
  66. Z. Xing, X. Zong, J. Pan and L. Wang, *Chemical Engineering Science*, 2013, **104**, 125-146.
  67. R. R. Jaini and T. F. Fuller, *International Journal of Hydrogen Energy*, 2014, **39**, 2462-2471.
  68. B. D. James, G. N. Baum, J. Perez and K. N. Baum, *Technoeconomic analysis of photoelectrochemical (PEC) hydrogen production*, 2009.
  69. M. R. Shaner, S. Hu, K. Sun and N. S. Lewis, *Energy & Environmental Science*, 2015, **8**, 203-207.
  70. K. Wu, Z. Chen, H. Lv, H. Zhu, C. L. Hill and T. Lian, *Journal of the American Chemical Society*, 2014, **136**, 7708-7716.
  71. K. Sun, F. H. Saadi, M. F. Lichterman, W. G. Hale, H.-P. Wang, X. Zhou, N. T. Plymale, S. T. Omelchenko, J.-H. He and K. M. Papadantonakis, *Proceedings of the National Academy of Sciences*, 2015, **112**, 3612-3617.
  72. Z. Li, W. Luo, M. Zhang, J. Feng and Z. Zou, *Energy & Environmental Science*, 2013, **6**, 347-370.
  73. D. K. Zhong, S. Choi and D. R. Gamelin, *Journal of the American Chemical Society*, 2011, **133**, 18370-18377.

74. J. A. Del Alamo, *Nature*, 2011, **479**, 317-323.
75. A. Murphy, P. Barnes, L. Randeniya, I. Plumb, I. Grey, M. Horne and J. Glasscock, *International journal of hydrogen energy*, 2006, **31**, 1999-2017.
76. A. Radi, D. Pradhan, Y. Sohn and K. T. Leung, *ACS nano*, 2010, **4**, 1553-1560.
77. S. K. Pilli, T. E. Furtak, L. D. Brown, T. G. Deutsch, J. A. Turner and A. M. Herring, *Energy & Environmental Science*, 2011, **4**, 5028-5034.
78. T. W. Kim and K.-S. Choi, *Science* 2014, **343**, 990-994.
79. F. F. Abdi, L. Han, A. H. Smets, M. Zeman, B. Dam and R. van de Krol, *Nature Communications*, 2013, **4**, 2195.
80. E. Rabinovich and G. Hodes, *The Journal of Physical Chemistry C*, 2013, **117**, 1611-1620.
81. J. R. Darwent and G. Porter, *Journal of the Chemical Society, Chemical Communications*, 1981, **4**, 145-146.
82. J. F. Reber and M. Rusek, *The Journal of Physical Chemistry*, 1986, **90**, 824-834.
83. K. Kalyanasundaram, E. Borgarello, D. Duonghong and M. Grätzel, *Angewandte Chemie International Edition in English*, 1981, **20**, 987-988.
84. M. F. Lichterman, A. I. Carim, M. T. McDowell, S. Hu, H. B. Gray, B. S. Brunshwig and N. S. Lewis, *Energy Environ. Sci.*, 2014, **7**, 3334-3337.
85. A. Pareek, R. Purbia, P. Paik, N. Y. Hebalkar, H. G. Kim and P. H. Borse, *International journal of hydrogen energy*, 2014, **39**, 4170-4180.
86. A. Pareek, P. Paik and P. H. Borse, *Langmuir*, 2014, **30**, 15540-15549.
87. S. Sakai, Y. Ueta and Y. Terauchi, *Japanese journal of applied physics*, 1993, **32**, 4413.
88. O. Khaselev, *Science*, 1998, **280**, 425-427.
89. S. Hu, M. R. Shaner, J. a. Beardslee, M. Lichterman, B. S. Brunshwig and N. S. Lewis, *Science*, 2014, **344**, 2547-2552.
90. K. Sun, Y. Kuang, E. Verlage, B. S. Brunshwig, C. W. Tu and N. S. Lewis, *Advanced Energy Materials*, 2015, **5**, 1402276.
91. K. Sun, F. H. Saadi, M. F. Lichterman, W. G. Hale, H.-P. Wang, X. Zhou, N. T. Plymale, S. T. Omelchenko, J.-H. He, K. M. Papadantonakis, B. S. Brunshwig and N. S. Lewis, *Proceedings of the National Academy of Sciences*, 2015, **112**, 3612-3617.
92. C. Li, T. Hisatomi, O. Watanabe, M. Nakabayashi, N. Shibata, K. Domen and J.-J. Delaunay, *Energy Environ. Sci.*, 2015, **8**, 1493-1500.
93. K. Sun, S. Shen, Y. Liang, P. E. Burrows, S. S. Mao and D. Wang, *Chemical reviews*, 2014, **114**, 8662-8719.
94. D. H. van Dorp, N. Hijnen, M. Di Vece and J. J. Kelly, *Angewandte Chemie International Edition*, 2009, **48**, 6085-6088.
95. A. Paracchino, N. Mathews, T. Hisatomi, M. Stefik, S. D. Tilley and M. Grätzel, *Energy & Environmental Science*, 2012, **5**, 8673-8681.
96. S. J. A. Moniz, S. A. Shevlin and D. J. Martin, *Visible-light driven heterojunction photocatalysts for water splitting – a critical review*, 2015, **8**, 731-759.
97. M. A. Mahmoud, W. Qian and M. A. El-Sayed, *Nano Letters*, 2011, **11**, 3285-3289.
98. L. Wu, L.-k. Tsui, N. Swami and G. Zangari, *The Journal of Physical Chemistry C*, 2010, **114**, 11551-11556.
99. A. Paracchino, V. Laporte, K. Sivula, M. Grätzel and E. Thimsen, *Nat Mater*, 2011, **10**, 456-461.
100. M. Wang, L. Sun, Z. Lin, J. Cai, K. Xie and C. Lin, *Energy & Environmental Science*,

- 2013, **6**, 1211-1220.
101. T. Jiang, T. Xie, L. Chen, Z. Fu and D. Wang, *Nanoscale*, 2013, **5**, 2938-2944.
  102. C.-Y. Lin, Y.-H. Lai, D. Mersch and E. Reisner, *Chemical Science*, 2012, **3**, 3482-3487.
  103. P. D. Tran, S. K. Batabyal, S. S. Pramana, J. Barber, L. H. Wong and S. C. J. Loo, *Nanoscale*, 2012, **4**, 3875-3878.
  104. Y. Hou, X. Y. Li, Q. D. Zhao, X. Quan and G. H. Chen, *Applied physics letters*, 2009, **95**, 093108.
  105. A. Paracchino, V. Laporte, K. Sivula, M. Grätzel and E. Thimsen, *Nature materials*, 2011, **10**, 456-461.
  106. C. G. Morales-Guio, S. D. Tilley, H. Vrubel, M. Grätzel and X. Hu, *Nature communications*, 2014, **5**, 3059.
  107. C. G. Morales-Guio, L. Liardet, M. T. Mayer, S. D. Tilley, M. Grätzel and X. Hu, *Angewandte Chemie International Edition*, 2015, **54**, 664-667.
  108. J. J. H. Pijpers, M. T. Winkler, Y. Surendranath, T. Buonassisi and D. G. Nocera, *Proceedings of the National Academy of Sciences*, 2011, **108**, 10056-10061.
  109. K. Sun, M. T. McDowell, A. C. Nielander, S. Hu, M. R. Shaner, F. Yang, B. S. Brunschwig and N. S. Lewis, *The Journal of Physical Chemistry Letters*, 2015, **2**, 592-598.
  110. M. J. Kenney, M. Gong, Y. Li, J. Z. Wu, J. Feng, M. Lanza and H. Dai, *Science*, 2013, **342**, 836-840.
  111. J. A. Turner, *Science*, 2012, **227**, 2012-2014.
  112. Y. W. Chen, J. D. Prange, S. Dühnen, Y. Park, M. Gunji, C. E. D. Chidsey and P. C. McIntyre, *Nature materials*, 2011, **10**, 539-544.
  113. M. T. McDowell, M. F. Lichterman, A. I. Carim, R. Liu, S. Hu, B. S. Brunschwig and N. S. Lewis, *ACS applied materials & interfaces*, 2015, **7**, 15189-15199.
  114. C. Shell, T. Photoanodes, R. H. Coridan, K. A. Arpin, B. S. Brunschwig, P. V. Braun and N. S. Lewis, *Nano Letters*, 2014, **14**, 2310-2317.
  115. X. Wang, K.-Q. Peng, Y. Hu, F.-Q. Zhang, B. Hu, L. Li, M. Wang, X.-M. Meng and S.-T. Lee, *Nano Letters*, 2013, **14**, 18-23.
  116. M. Shi, X. Pan, W. Qiu, D. Zheng, M. Xu and H. Chen, *International journal of hydrogen energy*, 2011, **36**, 15153-15159.
  117. S. C. Riha, B. M. Klahr, E. C. Tyo, S. n. Seifert, S. Vajda, M. J. Pellin, T. W. Hamann and A. B. Martinson, *ACS nano*, 2013, **7**, 2396-2405.
  118. S. S. K. Ma, K. Maeda, R. Abe and K. Domen, *Energy & Environmental Science*, 2012, **5**, 8390-8397.
  119. Q. Yu, X. Meng, T. Wang, P. Li and J. Ye, *Advanced Functional Materials*, 2015, **25**, 2686-2692.
  120. J. R. Galán-Mascarós, *ChemElectroChem*, 2015, **2**, 37-50.
  121. L. Liao, Q. Zhang, Z. Su, Z. Zhao, Y. Wang, Y. Li, X. Lu, D. Wei, G. Feng, Q. Yu, X. Cai, J. Zhao, Z. Ren, H. Fang, F. Robles-Hernandez, S. Baldelli and J. Bao, *Nature nanotechnology*, 2014, **9**, 69-73.
  122. Y. Surendranath, D. A. Lutterman, Y. Liu and D. G. Nocera, *Journal of the American Chemical Society*, 2012, **134**, 6326-6336.
  123. S. Y. Reece, J. A. Hamel, K. Sung, T. D. Jarvi, A. J. Esswein, J. J. H. Pijpers and D. G. Nocera, *Science*, 2011, **334**, 645-648.
  124. M. W. Kanan and D. G. Nocera, *Science*, 2008, **321**, 1072-1075.

125. Y. Kuang, Q. Jia, H. Nishiyama, T. Yamada, A. Kudo and K. Domen, *Advanced Energy Materials*, 2016, **6**, 1501645.
126. J. D. Blakemore, R. H. Crabtree and G. W. Brudvig, *Chemical Reviews*, 2015, **115**, 12974-13005.
127. X. Shi, I. Y. Choi, K. Zhang, J. Kwon, D. Y. Kim, J. K. Lee, S. H. Oh, J. K. Kim and J. H. Park, *Nat Commun*, 2014, **5**, 4775.
128. J. Wei, Y. Feng, P. Zhou, Y. Liu, J. Xu, R. Xiang, Y. Ding, C. Zhao, L. Fan and C. Hu, *ChemSusChem*, 2015, **8**, 2630-2634.
129. M. Gao, W. Sheng, Z. Zhuang, Q. Fang, S. Gu, J. Jiang and Y. Yan, *Journal of the American Chemical Society*, 2014, **136**, 7077-7084.
130. M. Dincă, Y. Surendranath and D. G. Nocera, *Proceedings of the National Academy of Sciences of the United States of America*, 2010, **107**, 10337-10341.
131. B. Klahr, S. Gimenez, F. Fabregat-Santiago, J. Bisquert and T. W. Hamann, *Journal of the American Chemical Society*, 2012, **134**, 16693-16700.
132. E. M. P. Steinmiller and K.-S. Choi, *Proceedings of the National Academy of Sciences of the United States of America*, 2009, **106**, 20633-20636.
133. C. Jiang, S. J. a. Moniz, M. Khraisheh and J. Tang, *Chemistry - A European Journal*, 2014, **20**, 12954-12961.
134. J. A. Seabold and K.-S. Choi, *Chemistry of Materials*, 2011, **23**, 1105-1112.
135. S. K. Choi, W. Choi and H. Park, *Physical chemistry chemical physics* 2013, **15**, 6499-6507.
136. C. L. Farrow, D. K. Bediako, Y. Surendranath, D. G. Nocera and S. J. Billinge, *Journal of the American Chemical Society*, 2013, **135**, 6403-6406.
137. D. K. Bediako, Y. Surendranath and D. G. Nocera, *Journal of the American Chemical Society*, 2013, **135**, 3662-3674.
138. D. J. Martin, P. J. T. Reardon, S. J. Moniz and J. Tang, *Journal of the American Chemical Society*, 2014, **136**, 12568 -12571.
139. M. Gong, Y. Li, H. Wang, Y. Liang, J. Z. Wu, J. Zhou, J. Wang, T. Regier, F. Wei and H. Dai, *Journal of the American Chemical Society*, 2013, **135**, 8452-8455.
140. L. Wang, F. Dionigi, N. T. Nguyen, R. Kirchgeorg, M. Gliech, S. Grigorescu, P. Strasser and P. Schmuki, *Chemistry of Materials*, 2015, **27**, 2360-2366.
141. M. Gong, Y. Li, H. Wang, Y. Liang, J. Z. Wu, J. Zhou, J. Wang, T. Regier, F. Wei and H. Dai, *Journal of the American Chemical Society*, 2013, **135**, 8452-8455.
142. Y. Kuang, Q. Jia, H. Nishiyama, T. Yamada, A. Kudo and K. Domen, *Advanced Energy Materials*, 2016, **6**, 1501645.
143. R. Memming, *Semiconductor electrochemistry*, John Wiley & Sons, 2008.
144. X. Zou and Y. Zhang, *Chemical Society Reviews*, 2015, **44**, 5148-5180.